

THEORETICAL INVESTIGATION OF MOLECULAR STRUCTURE, HOMO-LUMO, HYPERPOLARIZABILITY, NBO ANALYSIS AND DENSITY OF STATES CALCULATION OF BUTENAFINE

R.K.SANGEETHA^a, S. AYYAPPAN^{b,*}

^a*Department of Physics, Sri Eshwar College of Engineering, Coimbatore, India*

^b*Department of Physics, Government College of Technology, Coimbatore, India*

Molecular geometry vibrational wave number of butenafine was investigated using HartreeFock and DFT method with HF and B3LYP/6-31+G(d,p) basis set. The potential energy distribution of the vibrational wave number is found to be in good agreement with experimental values. A detailed NBO analysis of butenafine was done with B3LYP method. U-V visible absorption spectra of the titled molecule is calculated by PCM model using water as solvent. The U-V visible spectra of the titled molecule dissolved in water were recorded in the range of 200-900 nm. The calculated values of U-V spectra are the most reproduced experimental data. The density of states, Homo-lumo and electrostatic potentials were calculated and analyzed. The dipole moment and hyperpolarizability result shows the butenafine has non linear optical properties. The natural bonding analysis was calculated by HF and B3LYP method.

(Received September 28, 2019; Accepted February 18, 2020)

Keywords: DFT, HOMO-LUMO, Hyperpolarizability, UV-Visible, NBO, MESP

1. Introduction

The recent advances in medicine principally in antifungal therapy have introduced new fungicides, in order to reduce the antagonistic, invasive and therapeutic treatments. Ostensible fungal infections are common throughout the globe. There are three main anamorphic genera of dermatophyte, responsible for the group of infections generally known as tinea (namely Trichophyton, Microsporium and Epidermophyton). These infections are transmissible and transmitted via physical contact with arthroconidia, which are generated from dermatophyte filaments. Tinea infections affect the keratinised cells of the skin, hair and nails and are named according to the anatomical site infected. Trichophyton rubrum and Trichophyton mentagrophytes are the leading cause of tinea pedis, and tinea rubrum. Epidermophyton floccosum and tinea mentagrophytes are due to tinea cruris [1]. Butenafine [(4-tert-butylphenyl) methyl] (methyl) (naphthalen-1-ylmethyl) amine, a sole approved representative which belongs to the class of a phenol-substituted benzylamine derivatives was synthesized by Maeda et al. (T. Maeda, T. Arika, K. Amemiya, and K. Sasaki, Chem. Pharm. Bull., in press) has the molecular weight of 353.93 and an empirical formula $C_{23}H_{27}N.HCl$. It is an outstanding antifungal which possess a chemical structural arrangement indistinguishable to allylamine [2]. It works by killing sensitive fungi by interfering with the formation of the fungal cell membrane and weakening it. It has greater robustness when compared to azole derivatives and naftifine. Butenafine is slightly soluble in water, freely soluble in ethanol, methanol and chloroform, an effective antibiotic character of antifungal activity is visible; and is particularly active against dermatophytes, aspergilli, dimorphic fungi, and dematiaceous fungi (Maeda et al., in press). The desired result of butenafine was notably superior to those of tolnaftate, clotrimazole and bifonazole [3]. Several studies made explicit antimycotic and anti-inflammatory properties with butenafine. The current work deals with the theoretical calculation of hyperpolarizability, Homo-lumo and density of states of butenafine using the fundamental tools of computational technique so called density functional theory.

* Corresponding author: ayyappan@gct.ac.in

2. Computational details

The optimization of molecular structure of the titled molecule and the corresponding vibrational frequencies was calculated using HF and DFT with B3LYP/6-31+G(d,p) basis set using Gaussian software [4]. The geometrical structures of the title of the compound have been first optimized with full relaxation of potential energy and without any constraints and the geometry. The natural bonding analysis (NBO), hyperpolarizability, Homo-lumo and molecular electrostatic potential (MESP) were calculated by B3LYP/6-31+G(d,p) basis set [5]. The potential energy scanning (PES) of the titled molecule was calculated by using the same basis set. The density of state (DOS) is also estimated by B3LYP/6-31+G(d,p) method.

3. Results and discussion

3.1 Molecular geometrical structure analysis

The optimized bond length and bond angle in butenafine were determined using HF and DFT with B3LYP/6-31+G (d,p) basis set as listed in table (1) in accordance with atomic numbering scheme diagram as shown in figure (1). The total energy of the butenafine is obtained by RHF and RB3LYP as -941.3475 and -947.71068 Hartree respectively. The most of the optimized structure of the parameter such as bond length, bond angle and tetrahedral angles were also investigated by HF and B3LYP/6-31+G (d,p) basis set as presented. The benzene ring, naphthalene and CH₃ groups were noticeable in the titled molecule. The C₅-C₇, C₈-C₁₃ and C₃-C₆ bonds are occupied by larger bond length values when compared to the other C-C bond. This may be due to affect of substitution of nitrogen and methyl groups [6-9].

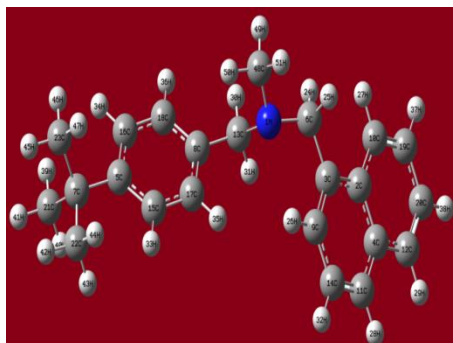


Fig. 1. Geometrical molecular structure of Butenafine.

The optimized bond angle of C-C in butenafine is in the range of 1.515Å – 1.378Å for aromatic ring and 1.539Å – 1.547Å for outside ring, while the initiation of substituent of methyl group causes a slight differences between the C-C bond length. The nitrogen present in between the two carbon atoms of the titled molecule and its N-C bond length value is 1.46 Å. The increase of the C-C bond length in the substituent is accompanied by slightly changes in bond angles C₅-C₁₆-C₁₈, C₈-C₁₇-C₁₅ and C₈-C₁₈-C₁₆ are 20.6°, 21.1° and 19.5° respectively.

Table. 1 Calculated bond length (Å), bond angle (°) and Dihedral angle (°) of butenafine using B3LYP/6-31+G(d,p) basis set.

Bond length(Å)		Bond angle(°)		Dihedral angle(°)	
Parameter	Value	Parameter	Value	Parameter	Value
N1-C6	1.464	C4-C12-H29	118.4	C2-C4-C11-C14	-0.4
N1-C13	1.468	C20-C12-H29	120.4	C2-C4-C11-H28	180.0
N1-C48	1.460	N1-C13-C8	113.8	C12-C4-C11-C14	179.2
C2-C3	1.434	N1-C13-H30	110.9	C12-C4-C11-H28	-0.4
C2-C4	1.435	N1-C13-H31	107.3	C2-C4-C12-C20	0.5
C2-C10	1.423	C8-C13-H30	109.0	C2-C4-C12-H29	-179.8
C3-C6	1.522	C8-C13-H31	109.1	C11-C4-C12-C20	-179.1
C3-C9	1.378	H30-C13-H31	106.5	C11-C4-C12-H29	0.6
C4-C11	1.418	C9-C14-C11	120.3	C15-C5-C7-C21	-121.1
C4-C12	1.419	C9-C14-H32	119.4	C15-C5-C7-C22	-0.9
C5-C7	1.539	C11-C14-H32	120.3	C15-C5-C7-C23	119.2
C5-C15	1.400	C5-C15-C17	121.6	C16-C5-C7-C21	59.3
C5-C16	1.402	C5-C15-H33	120.2	C16-C5-C7-C22	179.5
C6-H24	1.103	C17-C15-H33	118.2	C16-C5-C7-C23	-60.5
C6-H25	1.096	C5-C16-C18	120.6	C7-C5-C15-C17	-179.7
C7-C21	1.546	C5-C16-H34	119.9	C7-C5-C15-H33	0.3
C7-C22	1.540	C18-C16-H34	118.5	C16-C5-C15-C17	-0.1
C7-C23	1.547	C8-C17-C15	121.1	C16-C5-C15-H33	180.0
C8-C13	1.515	C8-C17-H35	119.3	C7-C5-C16-C18	179.6
C8-C17	1.396	C15-C17-H35	119.5	C7-C5-C16-H34	0.0
C8-C18	1.397	C8-C18-C16	121.2	C15-C5-C16-C18	-0.1
C9-C14	1.412	C8-C18-H36	119.5	C15-C5-C16-H34	-179.6
C9-H26	1.083	C16-C18-H36	119.4	C5-C7-C21-H39	-60.0
C10-C19	1.375	C10-C19-C20	119.5	C5-C7-C21-H40	60.3
C10-H27	1.082	C10-C19-H37	119.8	C5-C7-C21-H41	-179.9
C11-C14	1.371	C20-C19-H37	119.7	C22-C7-C21-H39	177.3
C11-H28	1.085	C12-C20-C19	119.8	C22-C7-C21-H40	-62.5
C12-C20	1.373	C12-C20-H38	120.3	C22-C7-C21-H41	57.3
C12-H29	1.085	C19-C20-H38	119.9	C23-C7-C21-H39	59.8
C13-H30	1.106	C7-C21-H39	111.8	C23-C7-C21-H40	-179.9
C13-H31	1.094	C7-C21-H40	110.9	C23-C7-C21-H41	-60.1
C14-H32	1.084	C7-C21-H41	110.3	C5-C7-C22-H42	180.0
C15-C17	1.393	H39-C21-H40	107.8	C5-C7-C22-H43	-60.8
C15-H33	1.082	H39-C21-H41	107.8	C5-C7-C22-H44	60.8
C16-C18	1.391	H40-C21-H41	108.2	C21-C7-C22-H42	-59.0
C16-H34	1.084	C7-C22-H42	109.6	C21-C7-C22-H43	60.1
C17-H35	1.084	C7-C22-H43	111.8	C21-C7-C22-H44	-178.2
C18-H36	1.086	C7-C22-H44	111.8	C23-C7-C22-H42	59.2
C19-C20	1.412	H42-C22-H43	107.6	C23-C7-C22-H43	178.4
C19-H37	1.084	H42-C22-H44	107.5	C23-C7-C22-H44	-60.0
C20-H38	1.084	H43-C22-H44	108.3	C5-C7-C23-H45	179.7
C21-H39	1.092	C7-C23-H45	110.4	C5-C7-C23-H46	59.8
C21-H40	1.093	C7-C23-H46	111.7	C5-C7-C23-H47	-60.5
C21-H41	1.095	C7-C23-H47	110.9	C21-C7-C23-H45	59.8
C22-H42	1.093	H45-C23-H46	107.8	C21-C7-C23-H46	-60.1
C22-H43	1.093	H45-C23-H47	108.1	C21-C7-C23-H47	179.6
C22-H44	1.093	H46-C23-H47	107.8	C22-C7-C23-H45	-57.6
C23-H45	1.095	N1-C48-H49	112.9	C22-C7-C23-H46	-177.6

Bond length(A°)		Bond angle(°)		Dihedral angle(°)	
Parameter	Value	Parameter	Value	Parameter	Value
C23-H46	1.092	N1-C48-H50	109.7	C22-C7-C23-H47	62.2
C23-H47	1.093	N1-C48-H51	109.7	C17-C8-C13-N1	-51.8
C48-H49	1.106	H49-C48-H50	108.0	C17-C8-C13-H30	-176.1
C48-H50	1.091	H49-C48-H51	108.3	C17-C8-C13-H31	68.0
C48-H51	1.092	H50-C48-H51	108.2	C18-C8-C13-N1	129.8
Bond angle(°)		Dihedral angle(°)		C18-C8-C13-H30	5.5
C6-N1-C13	111.0	C13-N1-C6-C3	-76.8	C18-C8-C13-H31	-110.4
C6-N1-C48	111.2	C13-N1-C6-H24	48.0	C13-C8-C17-C15	-178.3
C13-N1-C48	111.7	C13-N1-C6-H25	163.0	C13-C8-C17-H35	2.2
C3-C2-C4	118.9	C48-N1-C6-C3	158.2	C18-C8-C17-C15	0.2
C3-C2-C10	123.4	C48-N1-C6-H24	-77.0	C18-C8-C17-H35	-179.4
C4-C2-C10	117.7	C48-N1-C6-H25	38.0	C13-C8-C18-C16	178.2
C2-C3-C6	121.0	C6-N1-C13-C8	170.0	C13-C8-C18-H36	-1.9
C2-C3-C9	119.1	C6-N1-C13-H30	-66.7	C17-C8-C18-C16	-0.3
C6-C3-C9	119.8	C6-N1-C13-H31	49.2	C17-C8-C18-H36	179.6
C2-C4-C11	119.5	C48-N1-C13-C8	-65.3	C3-C9-C14-C11	0.3
C2-C4-C12	119.3	C48-N1-C13-H30	58.0	C3-C9-C14-H32	-179.7
C11-C4-C12	121.1	C48-N1-C13-H31	173.9	H26-C9-C14-C11	-179.7
C7-C5-C15	123.1	C6-N1-C48-H49	60.8	H26-C9-C14-H32	0.3
C7-C5-C16	120.0	C6-N1-C48-H50	-178.7	C2-C10-C19-C20	0.0
C15-C5-C16	116.9	C6-N1-C48-H51	-60.0	C2-C10-C19-H37	-180.0
N1-C6-C3	114.3	C13-N1-C48-H49	-63.8	H27-C10-C19-C20	179.5
N1-C6-H24	110.3	C13-N1-C48-H50	56.7	H27-C10-C19-H37	-0.4
N1-C6-H25	107.6	C13-N1-C48-H51	175.4	C4-C11-C14-C9	0.5
C3-C6-H24	110.2	C4-C2-C3-C6	178.4	C4-C11-C14-H32	-179.5
C3-C6-H25	108.2	C4-C2-C3-C9	1.3	H28-C11-C14-C9	-179.8
H24-C6-H25	105.9	C10-C2-C3-C6	-0.9	H28-C11-C14-H32	0.1
C5-C7-C21	109.5	C10-C2-C3-C9	-178.0	C4-C12-C20-C19	0.1
C5-C7-C22	112.4	C3-C2-C4-C11	-0.5	C4-C12-C20-H38	179.9
C5-C7-C23	109.4	C3-C2-C4-C12	179.9	H29-C12-C20-C19	-179.7
C21-C7-C22	108.1	C10-C2-C4-C11	178.8	H29-C12-C20-H38	0.1
C22-C7-C23	108.1	C3-C2-C10-C19	179.9	C5-C15-C17-H35	179.5
C13-C8-C17	121.4	C3-C2-C10-H27	0.3	H33-C15-C17-C8	180.0
C13-C8-C18	121.0	C4-C2-C10-C19	0.6	H33-C15-C17-H35	-0.5

The bond angle C-N-C value is 111° were estimated by B3LYP/6-31+G(d,p) basis set method. The nitrogen atoms are doped in between naphthalene and benzene groups so that the bond angles varying from 109.7°– 112.19° are affected by the exchange of electron density in between the two groups.

3.2 Dipole moment and Hyperpolarizability

The dipole moment and the first order hyperpolarizability were calculated by HF and B3LYP/6-31+G(d,p) basis set method[10,11]. The dipole moment and the first order hyperpolarizability of the titled molecules were calculated as shown in table(2). It can be seen that there is a additive contributions of diagonal polarizability [13]. The total dipole moment of butenafine for HF and B3LYP/6-31+G(d,p) method is 0.7768 Debye and 0.7194 Debye respectively. The mean first order hyperpolarizability of the title of molecule is predicted by HF and B3LYP method and the values are 0.83202×10^{-30} e.s.u and 0.72435×10^{-30} e.s.u respectively [14].It is observed that the dipole moment and the hyperpolarizability values are more appropriate for HF than the DFT method[15]. The mean hyperpolarizability of the butenafine is approximately

two times greater than hyperpolarizability of urea[16-18] .This values shows that there is a significant presence of the non linear optical properties of the butenafine.

Table 2. Calculated Dipole moment (μ) in Debye and hyperpolarizability (β) of butenafine by HF/6-31+G(d,p) and B3LYP/6-31+G(d,p) method.

μ value	HF/6-31+G(d,p)	B3LYP/6-31+G(d,p)
μ_x	-0.3376	-0.1677
μ_y	-0.6783	0.1139
μ_z	0.1226	0.19636
μ	-0.8933	0.14256
β value	HF/6-31+G(d,p)	B3LYP/6-31G+(d,p)
β_{xxx}	3.3064	12.0604
β_{yyy}	3.3371	82.4864
β_{zzz}	-8871	9.6420
β_{xvy}	25.0318	134.2059
β_{xxy}	8.8601	-2.9464
β_{xxz}	49.8579	29.7797
β_{xzz}	-13.7675	49.1429
β_{vzz}	-10.1864	13.8516
β_{vyz}	-14480	50.3614
β_{xvz}	9.2433	156.2073
Total	-23275.3173	534.7912
In e.s.u.	194.798×10^{-30}	4.476×10^{-30}

3.3. U-V Visible and Homo-lumo studies

The U-V visible spectra of the titled molecule is also been resolved. The absorption wavelength, excitation energy and oscillation strength were determined by time dependent density functional theory. The result coincides with the experimental findings values as shown in table(3).The absorption wavelength of the titled molecule calculated by TD-DFT/B3LYP/6-31+G(d,p) is 283nm that compliments to the experimental wavelength ($\lambda=287\text{nm}$) [19].The U-V visible analysis carries the major contribution energy among the Homo-Lumo and frontier orbital [20-21].

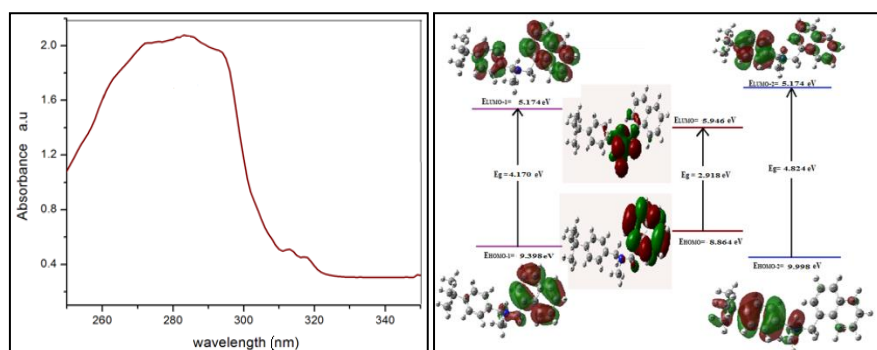


Fig.2. (a and b).Experimental UV-Vis absorbance spectra and Frontier Molecular diagram of Butenafine.

The energy gap between Homo- lumo depends on interaction between π and π^* interaction of the titled molecule. The electron absorption energy corresponding to the transition from the ground level to first excited state, that is one electron excitation exists from the highest occupying molecular orbital to lowest unoccupied molecular orbital. Generally, lowest unoccupied molecular orbital is π - bond nature[22].

Table 3. Experimental and computed absorption wavelength (λ), excitation energies (E) and oscillation strength (f) butenafine by B3LYP/6-31+G(d, p) method.

Exp wavelength (nm)	Theoretical wavelength (nm)	Excitation level	Transition state	Excitation energy(E) (eV)	Oscillation strength (f)
311	310	I	85→87 86→87	4.007	0.0186
	299	II	85→87 86→87	4.147	0.1892
287	283	III	83→87 85→88 86→88	4.3846	0.0040

The naphthalene group is delocalised over the whole C-C bonding interactions, so that Homo is located over the naphthalene groups of the titled molecule. Homo to Lumo transition implies an electron density transfer from aromatic ring part of π - conjugate system to the lone pair nitrogen atom [23]. The energy gap between the Homo- lumo is 2.918 eV. The Homo, lumo and frontier orbital energy transition level as shown in table(3). The lumo represents an electron acceptor and Homo represents the ability to donate electron as shown in energy level diagram in Figure(2.b).

3.4 Density of states

Total density of states and partial density of states were enumerated by using B3 LYP/6-31+ G(d,p) basis set. The total density of state (TDOS) and partial density of states (PDOS) of nitrogen, naphthalene group, methyl groups, benzene group and CH₂ group as shown in figure(3). DOS plot shows the population analysis in each orbital and demonstrates a simple view of the constitute molecular orbital in energy range from - 1.5 a.u. to +2.5 au. The partial density of states of CH₃ groups of the titled molecule is predominated to the naphthalene and benzene. At all the partial density of state , the energy distribution is through the energy line[24]. The density state value of nitrogen atom in this molecule is lower but the energy distribution is up to 2 a.u. as shown in figure (3). The positive value of OPDOS represents the bonding orbitals and the negative value represents the anti bonding orbitals. The negative value of OPDOS appears only in Lumo regions which is critical as observed. The density of states of the titled molecule is the energy distribution through carbon atom, than the other atoms such that the density of states of carbon is predominant in this molecule[25].

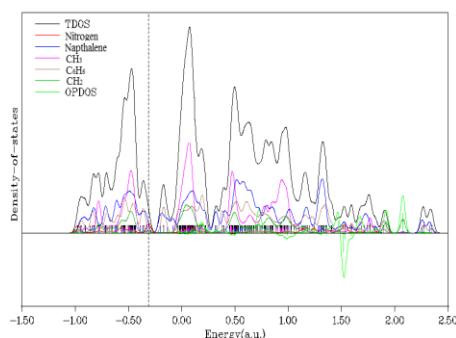


Fig.3. Total and partial density of states diagram of Butenafine.

3.5. Natural Bonding Orbitals Analysis

Natural Bonding Orbital analysis provides the most accurate and possible Maxwell Lewis structure and highest percentage of density of orbital. It enhances the analysis of inter and intra molecular interactions based on interaction between filled and virtual orbital of the titled molecule[29]. The second order Perturbation theory analysis of Fock matrix evaluates the donor and acceptor from the NBO analysis of the titled molecule. The result of interaction is loose occupants from the concentration of electrons in the Lewis structure into the empty non Lewis structure[30]. The NBO analysis also describes the bonding intense of the natural hybrid orbital system. The bonding N_1-C_6 , N_1-C_{13} and N_1-C_{48} is 1.980 interacts with anti bonding C_3 and C_8 stabilization energy values are 13579, 12890 and 15384 kcal/mol. The bonding $C_{22}-H_{44}$ (1.9889) interacts with C_{48} (0.0002) with stabilization energy 90391 kcal/mol, where as high stabilization energy predicts as relatively high charge transfer from one methyl group to another methyl group of carbon[31]. From the NBO analysis table(4), the C-C interaction is very stronger than the C-N interaction. The molecular stabilization depends on the C-C interactions and the stabilization energy calculated based on NBO analysis is shown in table(4).

Table 4. Second Order perturbation theory analysis of Fock matrix in NBO basis for butenafine by B3LYP/6-31+G (d, p) method.

Donor (i)	ED/e	Acceptor (j)	ED/e	E(2) kcal/mol	E(j)-E(i) a.u.	F(i,j) a.u.
N1 - C 6	1.9881	C3	0.0001	13579	0.02	0.495
N1 - C13	1.9802	C 3	0.0001	12890	0.01	0.332
N1 - C48	1.9860	C8	0.0067	15384	0.02	0.521
C4 - C12	1.9698	C22 - H44	0.0066	3067	0.06	0.394
C 5 - C16	1.9709	C22 - H 44	0.0066	5418	0.04	0.42
C6 - H25	1.9673	C 16 - H34	0.0323	1580	0.06	0.281
C10 - C19	1.9793	H26	0.0008	1365	0.63	0.882
C10 - C19	1.9793	C 7 - C 23	0.2354	17533	0.03	0.676
C11 - H28	1.9795	N1	0.0004	216	3.1	0.733
C11 - H28	1.9795	C6	0.0001	12260	0.21	1.453
C11 - H28	1.9795	C21 - H40	0.0060	2552	0.36	0.858
C12 - C20	1.9774	C48	0.0000	1196	0.1	0.309
C12 - C20	1.9774	C22 - H44	0.0066	1264	0.05	0.225
C13 - H30	1.9859	C 8	0.0067	32547	0.01	0.591
C13 - H 31	1.9705	C15 - C17	0.0149	1175	0.03	0.163
C18 - H36	1.9798	C3	0.0001	19336	0.03	0.738
C18 - H36	1.9798	C 8 - C18	0.0233	5807	0.06	0.526
C19 - C20	1.9781	C2	0.0001	67017	0.32	4.125
C19 - C20	1.9781	H25	0.0005	29704	0.38	2.997
C19 - C20	1.9781	C15 - C17	0.0149	1378	2.97	1.809
C19 - H37	1.9806	C8	0.0067	8986	0.04	0.541
C21 - H40	1.989	C48	0.0022	10971	0.26	1.514
C22 - H44	1.9889	C10	0.0007	31274	2.21	7.439
C 22 - H44	1.9889	C11 - H28	0.0147	10953	3.49	5.528
N1	1.9994	C48	0.0001	3409	2.5	2.604
N1	1.9994	H51	0.0001	2800	3.13	2.642
N1	1.9994	C9 - C14	0.0167	929	6.13	2.139
C11	1.9988	H51	0.0002	13257	0.21	1.484
C11	1.9988	C9 - C14	0.0167	935	2.23	1.294

3.6. The potential energy surface scanning

The potential energy surface scanning is performed by Gaussian software using DFT/B3LYP/ 6-31+G(d,p) level of approximations. The $C_8-C_{13}-N_1-C_{48}$ and $C_3-C_6-N_1-C_{48}$ dihedral angles varies in steps of 10° to 360° . Two minimum energy curve has been obtained for $C_8-C_{13}-N_1-C_{48}$ at angle of 130° and 270° in the potential energy curve as shown in figure(5). The

maximum potential of the titled molecule obtained is at 70° and 210° respectively[32]. The two minimum potential energy values of the titled molecule is -1408.53887 Hartree and the two maximum potential value is -1408.52705 Hartree.

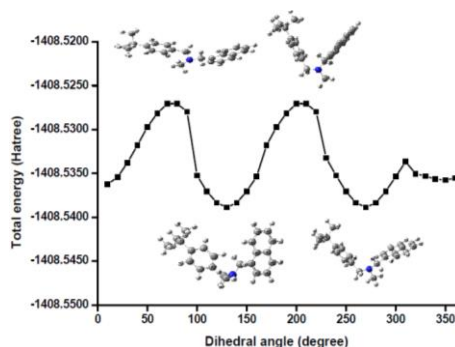


Fig. 5. Potential energy surface scanning diagram of Butenafine.

3.7. Thermal properties

The steady state thermodynamic function such as heat capacity, entropy, change in enthalpy for the butenafine molecule were obtained from B3LYP/6-31+G(d,p). The thermal parameters values are calculated with respect to change in temperature. The steady state thermodynamic function of the titled molecule increases with increasing temperature ranging from 100K to 1000 K as shown in Fig. 6.

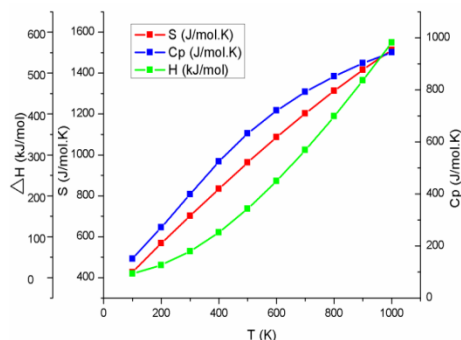


Fig.6. The graph drawn between Temperature vs entropy(S), change in Enthalpy(ΔH) and heat capacity (C_p) diagram of Butenafine.

The steady state thermodynamic function [33-34]are fitting in equations are given below

$$\begin{aligned} S &= 335.43 + 15.111T + 2.435 \times 10^{-2}T^2 \\ C_p &= 128.5 + 35.9123T + 5.788 \times 10^{-2}T^2 \\ \Delta H &= -114 + 25.1268T + 4.05 \times 10^{-2}T^2 \end{aligned}$$

The correlation equation between the heat capacity, entropy and change in enthalpy with temperature were fitted by quadratic equations and their corresponding R^2 values are 0.96333, 0.99638 and 0.96513 respectively. The steady state thermodynamic data of the title molecule is helpful for the further studies of the molecules.

4. Conclusions

We have carried out HF and B3LYP/6-31+G (d, p) method along with the structure and geometrical parameters of butenafine using B3LYP/6-31+G (d, p) basis set method. The electronic transitions have been calculated in the water environment using PCM model, TD-DFT/B3LYP/6-31+G(d,p) shows the charge transfer within the molecule.

The Homo-lumo of the butenafine illustrates more clearly about the involvement of density of charge transfer between the acceptor and donor groups. The density of states of the butenafine is also studied. The change in thermodynamic parameters relates heat capacity, entropy and enthalpy with changing temperature. The correlations between the thermodynamic parameters and temperatures are obtained.

References

- [1] T. A. Syed et al., *Tropical Medicine & International Health* **4**(4), 284 (1999).
- [2] T. Arikaet al., *Antimicrobial agents and chemotherapy* **34**(11), 2254 (1990).
- [3] Eduardo Tschenet al., *Journal of the American Academy of Dermatology* **36**(2), S9 (1997).
- [4] Gaussian 09, Revision A.02, M. J. Frisch, G. W. Trucks, H. B. Schlegel et al, Gaussian, Inc., WallingfordCT, 2016.
- [5] Fahmi Himoet al., *Journal of the American Chemical Society* **127**(1), 210 (2005).
- [6] Tatsuhiko Sagara, James Klassen, Eric Ganz, *The Journal of chemical physics* **121**(24), 12543 (2004).
- [7] David M. Deaven, Kai-Ming Ho, *Physical review letters* **75**(2), 288 (1995).
- [8] Warren J. Hehre, Wiley-Interscience, 1986.
- [9] Ronald J. Gillespie, István Hargittai, Courier Corporation, 2013.
- [10] S. R. Marder, D. N. Beratan, L. T. Cheng. *Science* **252**(5002), 103 (1991).
- [11] Larry R. Dalton, Aaron W. Harper, Bruce H. Robinson, *Proceedings of the National Academy Of Sciences* **94**(10), 4842 (1997).
- [12] Giovanni Ciccotti, Mauro Ferrario, J-P. Ryckaert. *Molecular Physics* **47**(6), 1253 (1982).
- [13] M. Blanchard-Desce et al., *Chemistry—A European Journal* **3**(7), 1091 (1997).
- [14] D. Sajanet al., *Journal of Molecular Structure* **785**(1), 43 (2006).
- [15] S. J. A. Van Gisbergen, J. G. Snijders, E. J. Baerends, *Physical Review Letters* **78**(16), 3097 (1997).
- [16] Stephan P. A. Sauer, *Journal of Physics B: Atomic, Molecular and Optical Physics* **30**(17), 3773 (1997).
- [17] P. Norman, D. M. Bishop, H. J. A. Jensen, J. Oddershede, *The Journal of chemical physics* **123**(19), 194103 (2005).
- [18] Benoît Champagne et al., *The Journal of chemical physics* **122**(11), 114315 (2005).
- [19] R. R. Meier, *Space Science Reviews* **58**(1), 1 (1991).
- [20] Vincent Lavallo et al., *Angewandte Chemie* **118**(21), 3568 (2006).
- [21] Jun-ichi Aihara, *The Journal of Physical Chemistry A* **103**(37), 7487 (1999).
- [22] Shlomo Alexander, Raymond Orbach, *Journal de Physique Lettres* **43**(17), 625 (1982).
- [23] G. Lehmann, M. Taut, *Physica Status Solidi B* **54**(2), 469 (1972).
- [24] C. H. Suresh, Nobuaki Koga, *Inorganic chemistry* **41**(6), 1573 (2002).
- [25] Cherumuttathu H. Suresh, *Inorganic chemistry* **45**(13), 4982 (2006).
- [26] Alan E. Reed, Frank Weinhold, *The Journal of Chemical Physics* **78**(6), 4066 (1983).
- [27] J. E. Carpenter, F. Weinhold, *Journal of Molecular Structure: Theochem* **169**, 41 (1988).
- [28] Alan E. Reed et al., *The Journal of Chemical Physics* **84**(10), 5687 (1986).
- [29] P. Bobadova-Parvanova et al., *The Journal of chemical physics* **116**(9), 3576 (2002).
- [30] Alexander A. Balandin, *Nature materials* **10**(8), 569 (2011).
- [31] Khan M. F. Shahil, Alexander A. Balandin, *Solid State Communications* **152**(15), 1331 (2012).